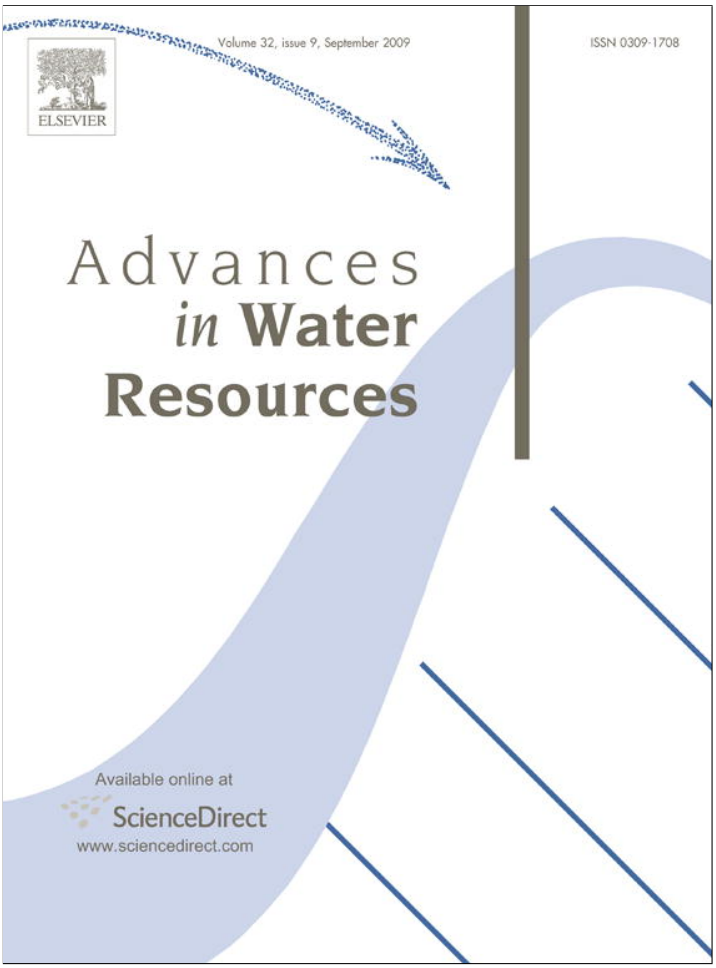

Advances in Water Resources 32 (2009) 1444–1459

Contents lists available at ScienceDirect

Advances in Water Resources

journal homepage: www.elsevier.com/locate/advwatres

Simulating daily, monthly and annual water balances in a land surface model using alternative root water uptake schemes

Mustapha El Maayar [a,*], David T. Price [b], Jing M. Chen [a]

[a] Department of Geography and Program in Planning, University of Toronto, 100 St. George Street, Toronto, Ontario, Canada M5S 3G3
[b] Natural Resources Canada, Canadian Forest Service, Edmonton, Alberta, Canada

ARTICLE INFO

Article history:
Received 27 September 2006
Received in revised form 3 July 2009
Accepted 6 July 2009
Available online 15 July 2009

Keywords:
Root water uptake
Water balance
Land surface models

ABSTRACT

Hydrological simulations at multi-temporal time scales by a widely used land surface model (LSM) are investigated under contrasting vegetation and meteorological conditions. Our investigation focuses particularly on the effects of two different representations of root water uptake and root profile on simulated evapotranspiration (ET) and soil moisture by the Integrated BIosphere Simulator (IBIS). For this purpose, multi-year eddy covariance measurements, collected at four flux-tower sites across North America, were used to gauge IBIS simulations with: (a) its standard version (IBIS2.1), in which static root water uptake (RWU) and root profile schemes are incorporated; and (b) a modified version in which dynamic RWU and root profile schemes replaces the static schemes used in the standard version. Overall, our results suggest that the modified version of the model performs more realistically than the standard version, particularly when high atmospheric demand for evaporation is combined with high atmospheric vapour pressure deficit and low soil water availability. The overall correlation between simulated and measured monthly ET rates at the simulated sites reached 0.87 and 0.91 for the standard and the modified versions, respectively. Our results also show that the incorporation of the dynamic RWU in IBIS yields improved simulations of ET under very dry conditions, when soil moisture falls down to very low levels. This suggests that adequate representations of vegetation responses to drought are needed in LSMs as many state of the art climate models projections of future climate indicate more frequent and/or more intense drought events occurring in some regions of the globe. Our analysis also highlighted the urgent need for adequate methodologies to correct field measurements that exhibit energy imbalances in order to provide rigorous assessments of land surface model simulations of heat and mass exchanges between the land surface and the atmosphere.

1. Introduction

Adequate simulations by land surface models (LSMs) of the Earth's surface hydrological processes at multiple spatio-temporal scales is one of the most challenging issues in modern environmental science. In particular, correct partitioning among the various components of the water budget is important for several reasons, including reliable climate predictions [41], the investigation of land use change on small and large hydrological basins [44,45], the enhancement of Earth's water resources management strategies [16], the improvement of global and regional estimations of pollutant transport by rivers [22,62], the quantification of the separate effects of human land use and climate variability on potential future global and regional scarcity of fresh water resources [63], and potentially, to help avoid conflicts over water resources between neighboring countries [5,58]. Unsurprisingly then, an important research focus has been, for more than a decade, the improvement of hydrological simulations in LSMs [10,17,18,23,26,51,56,64].

Several approaches have been developed over the last three decades to model land surface water budgets [43,64,29,44]. The current diversity of schemes to represent terrestrial hydrology ranges from purely simple empirical models to process-oriented models that incorporate detailed descriptions of soil and canopy physics. The latter class is generally recognized to be the most suitable for investigating land surface hydrology, and its responses to climate variability [2,43]. Moreover, several recent studies have suggested that better representations of root water uptake and root profile are needed within existing hydrological models to better capture the effects of vegetation on surface hydrology [4,13,21,28,29,37].

The Integrated BIosphere Simulator (IBIS) is an LSM that incorporates a physically based approach to simulate land surface hydrology [30]. It is a dynamic vegetation model, where canopy and soil physics are simulated using the LSX Soil-Vegeta-

* Corresponding author. Tel.: +1 416 946 3058; fax: +1 416 946 3886.
E-mail address: elmaayarm@geog.utoronto.ca (M. El Maayar).

0309-1708/$ - see front matter © 2009 Elsevier Ltd. All rights reserved.
doi:10.1016/j.advwatres.2009.07.002

Table 1
Values of λ as given in Li et al. [5].

Case	θ_a in the upper 1/3 depth	θ_a in the lower 2/3 depth	λ
1	<0.2	>0.5	0.50
2	<0.2	0.2–0.5	0.75
3	0.2-0.5	>0.5	0.75
4	0.2-0.5	<0.2	1.25
5	>0.5	0.2–0.5	1.25
6	>0.5	<0.2	1.50
Others			1.00

Table 2
Values of b and calculated K as a function of soil texture. K was calculated following the procedure explained in Campbell and Norman [12, Chapter 9].

Soil texture class	b	K
Sand	1.7	19.91
Loamy sand	2.1	9.97
Sandy loam	3.1	3.19
Loam	4.5	1.85
Silt loam	4.7	1.50
Sandy clay loam	4.0	1.91
Clay loam	5.2	1.35
Silty clay loam	6.6	0.92
Sandy clay	6.0	1.13
Silty clay	7.9	0.75
Clay	7.6	0.81

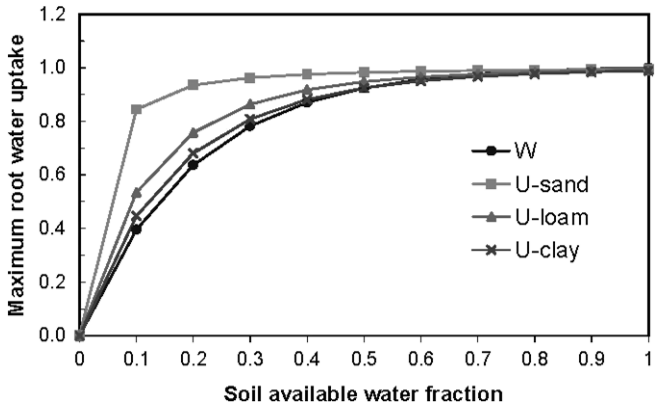

Fig. 1. Maximum root water uptake as modeled in standard and modified versions of IBIS (IBIS-st and IBIS-mod, respectively). W is the generic soil maximum soil water uptake algorithm used in IBIS-st, while the U traces are new soil texture-dependent formulations (See Eqs. (5) and (12), respectively).

tion–Atmosphere-Transfer scheme [52], coupled to a carbon exchange module [30]. Recently, Li et al. [45, hereafter referred to as L05] proposed a new representation of the soil water stress effect on plant transpiration simulated by IBIS, which improved annual runoff simulations in two basins located in West Africa. That is, the L05 study showed potential as a general improvement of hydrological simulations within IBIS. Nevertheless, validation of the new scheme is still needed for two main reasons. Firstly, L05 did not address the effects of their new representation on root water uptake (RWU) by vegetation, and hence on canopy evapotranspiration. Secondly, proper validation generally requires field measurements collected from a range of contrasting environmental conditions, and over multiple temporal scales.

The objective of this study is to compare the performance of the standard version of IBIS (IBIS-st) [30,42], with a new version (IBIS-mod) that incorporates a slightly modified form of the L05 scheme coupled to a rooting depth scheme suggested recently by Arora and Boer [4]. The validation data are multi-year field measurements of soil moisture and evapotranspiration, collected at several eddy covariance measurement sites in the Fluxnet research network established across North America (http://www.fluxnet.ornl.gov/fluxnet/index.cfm). These sites were selected to be representative of a wide range of vegetation types and environmental conditions, including boreal and temperate broadleaf forests, a temperate coniferous forest, and a warm grassland ecosystem.

2. Description of IBIS's hydrological module

2.1. Original model

IBIS enables the simulation of ecosystem processes that operate at different time scales (ranging from minutes/hours to years) within a single framework. These processes include soil and canopy physics, canopy physiology, vegetation phenology, soil biogeochemistry, and long-term vegetation dynamics (competition, mortality, large-scale disturbances). The model simulates six soil layers of a total depth of 6 m. Going from the surface to the bottom soil depth, layer thicknesses are 10 cm (0–10 cm), 15 cm (10–25 cm), 25 cm (25–50 cm), 50 cm (50–100 cm), 100 cm (100–200 cm) and 200 cm (200–400 cm), respectively. Here, we describe only IBIS's hydrological component. Complete descriptions of the model can be found in Foley et al. [30] and Kucharik et al. [42].

In IBIS, as in many land surface models, vertical soil water movement is simulated according to Richards' equation for unsaturated flow which combines Darcy's Law and the mass continuity equation [12,65]. Thus, the instantaneous vertical variation in volumetric soil moisture content, θ, is expressed as:

$$\frac{\partial \theta}{\partial t} = \frac{\partial}{\partial z}\left(D\frac{\partial \theta}{\partial z}\right) + \frac{\partial K}{\partial z} - S(t,z), \quad (1)$$

where D is the vertical soil water diffusivity, K is the hydraulic conductivity, and $S(t,z)$ is the sink term. The terms t and z (positive upward) represent the time and space coordinates, respectively, hence $S(t,z)$ represents water uptake by roots, which equates total plant

Table 3
Key ecological, climatic, and soil conditions at the experimental sites that were selected for our study. For temperature and precipitation, shown values are 1961–1990 normals.

	Campbell River (BC, Canada)	BOREAS-SSA (SK, Canada)	Walker branch watershed (TN, USA)	Little Washita watershed (OK, USA)
Symbol	CR	SOA	WBW	LW
Vegetation type	Temperate coniferous (mature Douglas-fir forest)	Boreal broadleaf deciduous forest (old aspen)	Temperate broadleaf deciduous forest (mature oak)	Warm (C4) tall grasses
Geographical coordinates (latitude/longitude)	49.87 N/125.34 W	53.63 N/ 106.20 W	35.96 N/ 84.29 W	34.96 N/96.68 W
Elevation (m)	300	601	365	500
Mean temperature (°C)	9.4	−0.4	13.9	16.1
Annual precipitation (mm)	1369	368	1355	805
Soil texture	Sandy	Silty loam	Silty loam	Clay loam
Maximum LAI	6.7	4.5	6	3
Canopy height (m)	33	21	25	0.5

transpiration (T). In IBIS, T is calculated as the sum of transpiration rates from each of upper and lower vegetation canopy layers, while transpiration from each layer is calculated as:

$$T_{vl} = \frac{\rho s_{vl}}{(1 + r_{vl} s_{vl})} (1 - f_{vl}^{wet}) [q_{sat}(T_{leaf,vl}) - q_{vl}] L_{vl}, \quad (2)$$

where ρ (kg m^{-3}) is the dry air density near the surface, s (m s^{-1}) is a vegetation-atmosphere heat transfer coefficient, f^{wet} is the wet fraction of leaf area index (liquid or snow), r (s m^{-1}) is the stomatal resistance, q_{sat} (kg kg^{-1}) is the specific humidity of the air within the canopy, T_{leaf} is the leaf temperature, and L is the single sided leaf area index. The subscript vl denotes either upper or lower vegetation layers.

For a given soil layer i, root water uptake, RWU_i (kg [H_2O] m^{-2} s^{-1}), is calculated in IBIS as the product of plant transpiration, T (kg [H_2O] m^{-2} s^{-1}), and the water uptake fraction, F_i, as:

$$RWU_i = T \cdot F_i, \quad (3)$$

where F_i is a function of both root distribution and soil water availability, W, given by:

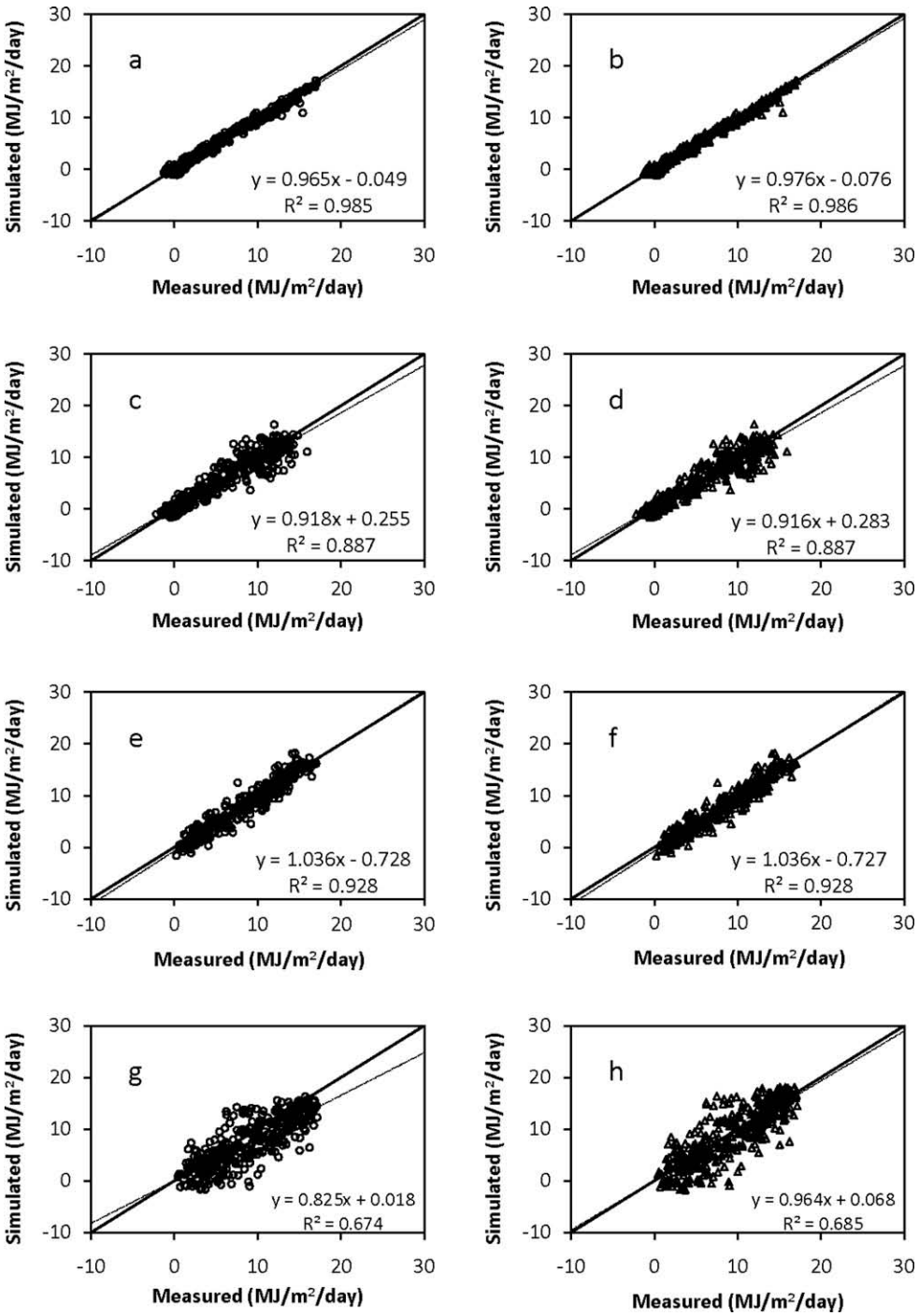

Fig. 2. Simulated versus measured (1:1 line) daily net radiation. Simulations in the left (circles) and right (triangles) panels correspond to standard and modified versions simulations, respectively. a and b: CR-Douglas-fir forest; c and d: SOA-old aspen forest; e and f: WBW-oak forest; g and h: LW-warm grasses. The dotted thin line corresponds to the equations shown on figures ($y = f(x)$).

Table 4
Average daily net radiation statistics at the selected four sites. Average and standard deviations (*std*) values are given in (MJ m^{-2} day^{-1}). MBE is the absolute mean bias error, and S1 and S2 refer to the simulations with the standard and the modified versions of the model, respectively. p is the probability value for the two-tailed Student's t-test.

	CR	SOA	WB	LW
Measured	6.42	5.48	8.25	8.97
Simulated-S1	6.05	5.23	7.76	7.37
Simulated-S2	5.94	5.25	7.76	8.66
std-Measured	5.41	5.21	4.69	4.73
std-Simulated-S1	5.12	4.92	4.90	4.63
std-Simulated-S2	5.00	4.92	4.90	5.37
Correlation-1 (r)	0.99	0.94	0.96	0.82
Correlation-2 (r)	0.99	0.94	0.96	0.83
MBE-1 (%)	5.17	4.64	5.94	17.79
MBE-2 (%)	4.55	4.30	5.90	3.46

$$F_i = \frac{R_i W_i}{\sum_{j=1}^{n} R_j W_j}, \tag{4}$$

where n is the number of soil layers, R_i is the fraction of total root biomass present in layer i and W is defined as:

$$W = \frac{1 - e^{sf \cdot \theta_a}}{1 - e^{sf}}, \tag{5}$$

where sf, set to -5 in IBIS, is an empirical factor that adjusts the effect of soil water stress on plant photosynthesis, and θ_a is the available water fraction calculated from θ, wilting point, θ_{wp}, and field capacity, θ_{fc}, as:

$$\theta_a = \frac{\theta - \theta_{wp}}{\theta_{fc} - \theta_{wp}}. \tag{6}$$

In each soil layer i, R_i in Eq. (4) is calculated as the difference between the cumulative fractions of root biomass from soil surface in layers i (Y_i) and $i-1$ (Y_{i-1}), as:

$$R_i = Y_i - Y_{i-1}. \tag{7}$$

Y is represented using the asymptotic equation of Gale and Grigel [31], as:

$$Y = 1 - \beta^d, \tag{8}$$

where d (cm) represents the soil depth containing plant roots, and β is a factor that determines the root distribution within that depth. Eq. (8) suggests that large β (e.g., 0.99) results in a large proportion of roots deep in the soil, while low β (e.g., 0.90) results in more roots closer to the soil surface. IBIS uses the compilation of Jackson et al. [36] to define biome-specific β values.

Finally, the total soil water stress exerted through all plant roots, S_{ws}, is calculated as:

$$S_{ws} = \sum_{i=1}^{n} R_i W_i. \tag{9}$$

2.2. Modified model

2.2.1. Root water uptake

Root water extraction as described in IBIS-st, and pointed-out in L05, ignores the tendency for plant roots to exploit wetter layers when high stress is encountered in dry layers. Several field observations lend support to this argument. Kljun et al. [40] and Prihodko et al. [53] both reported that to maintain photosynthesis, vegetation tends to use deep soil water when near soil surface dries out. Canadell et al. [13] reported that under extreme dry conditions such as those observed in the Kalahari desert, some species are able to grow roots as deep as 68 m to extract water. Earlier work showed that plants extract water preferentially from wetter layers to optimize their use of available energy [54]. Thus, L05 proposed a new scheme in which a dynamic allocation of root water uptake is simulated to compensate for the stress effect exerted by dry soil layers by increasing water uptake from wetter layers.

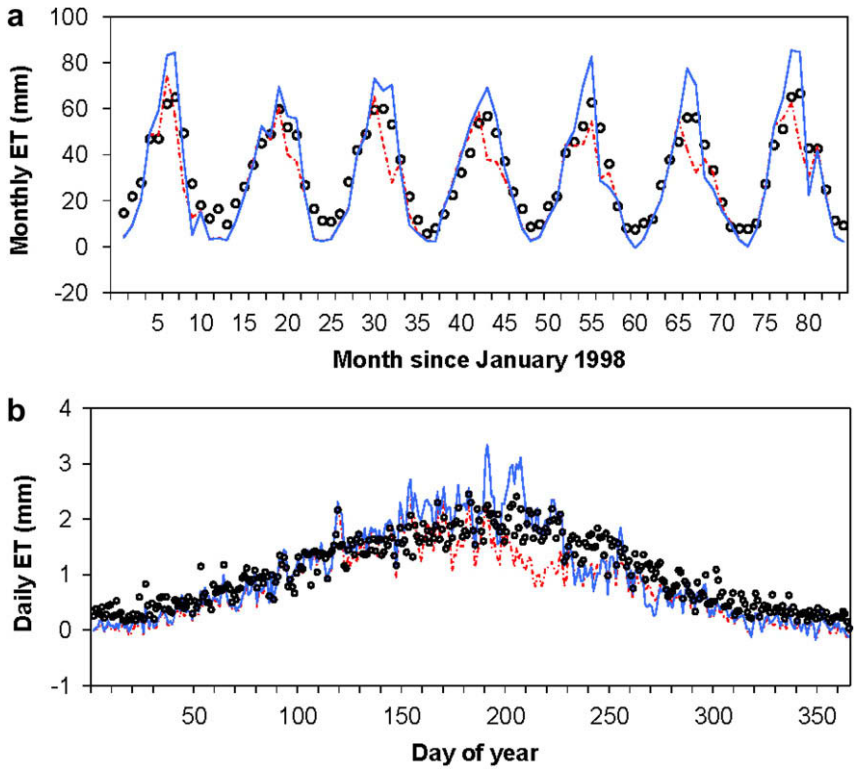

Fig. 3. Seasonal variation of simulated and measured ET at the CR site. (a) Monthly variation; (b) average daily variation over the entire period of the simulations (1998–2004). Dots, dotted lines and solid lines refer to measured, standard and modified IBIS simulations, respectively.

In their new scheme, L05 describe the root water uptake fraction, F_i, from a given layer i as:

$$F_i = \frac{R_i^{\lambda} W_i}{\sum_{j=1}^{n} R_j^{\lambda} W_j}. \quad (10)$$

In Eq. (10), the relative importance of water uptake by roots found in each soil layer is determined by the λ parameter. To allow for a dynamic adjustment of root water uptake by the vegetation, L05 suggested the use of an λ exponent that varies with the vertical soil moisture distribution (see also [46]). Thereafter, a compilation of field observations has served to select the appropriate λ values (Table 1). The total soil water stress, S_{ws}, is then expressed as the product of F_i and the maximum water that the vegetation can extract from each layer i, U_i, as a function of soil hydrologic constraints:

$$S_{ws} = \sum_{i=1}^{n} F_i U_i. \quad (11)$$

Here, U is expressed according to [12], as:

$$U = 1 - (1 + K \cdot \theta_a)^{-b}, \quad (12)$$

where the exponent b (dimensionless) is the soil moisture release parameter, that varies with soil texture [12]. L05 used a generic value for K (1.3) for all soil types. In reality, however, K is a critical parameter that is strongly influenced by soil texture. A more realistic approach to express U is therefore to calculate K as a function of soil texture, as suggested in [12]. Values of b and our values of K calculated according to [12] are given in Table 2.

Eqs. (5), (9), (11) and (12) indicate that an additional important difference between the two root water uptake schemes, described above, is related to the maximum water that vegetation is able to extract from the soil. These maximums are controlled by W in IBIS-st and by U in IBIS-mod, while a comparison of their variation as a function of the soil water content is illustrated in Fig. 1. It is shown that for all soil textural classes, the maximum RWU is larger in IBIS-mod than in IBIS-st.

2.2.2. Rooting depth and root profile

A further modification consists of taking plant age into account to derive the rooting depth and the root distribution profile within the soil, using a relationship suggested by Arora and Boer [4]. In that relation, the root biomass, which depends upon the age of the vegetation (either prescribed in the vegetation type, or simulated dynamically), is used to derive the vertical profile of the roots within the soil system, from:

$$RD = \frac{3}{a}, \quad (13)$$

where RD is the rooting depth (defined as the depth in which 95% of plant roots are found); and a is a parameter linked to root biomass density, $B(t)$ (kg m^{-2}), as follows:

$$a = C/[B(t)]^{\alpha}, \quad (14)$$

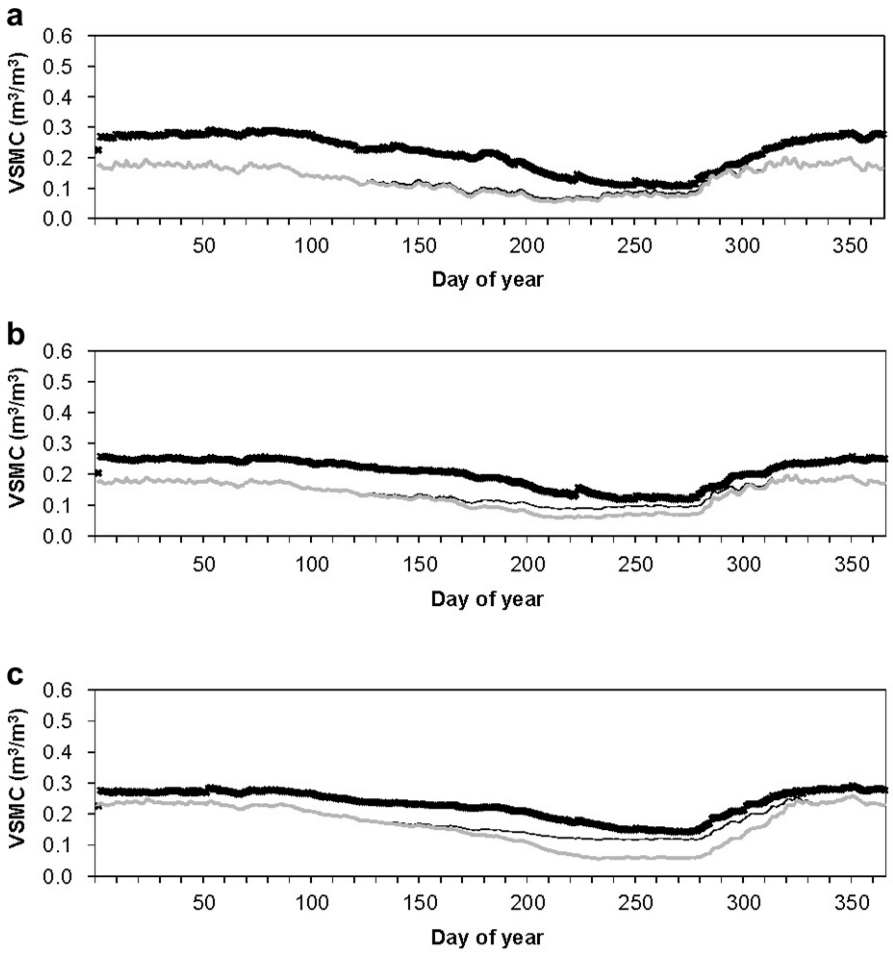

Fig. 4. Simulated and measured seasonal variation of volumetric soil moisture content (VSMC) at the CR site. Shown are average daily variations over the entire period of the simulations (1998–2004). Crosses (Thickest dark line), thin solid line and thick gray solid line refer to measured, standard and modified IBIS simulations, respectively. (a) 0–30 cm; (b) 0–60 cm; (c) 0–100 cm.

where α is the root growth direction parameter that determines the main direction of root development (horizontal vs. vertical). The root distribution profile of Jackson et al. [36] as used in IBIS-st is obtained when α is set to zero. However, from a range of field observations of root profiles and root biomass densities, Arora and Boer [4] found that 0.8 constitutes a reasonable approximation for α under most conditions. Parameter C is a biome-specific constant value derived as:

$$C = \bar{a}(\overline{B})^{\alpha}, \tag{15}$$

where $\bar{a}$ is a parameter that represents the typical root distribution profile and $\overline{B}$ represents the typical root biomass density (kg C m^{-2}).

3. Site locations and data

3.1. Sites information

Simulations of IBIS-st and IBIS-mod were compared for a humid temperate coniferous forest located on the west coast of Canada (mature Douglas-fir), a mature boreal broadleaf deciduous forest located in the boreal forest of central Saskatchewan (BOREAS southern old aspen site), a mature temperate broadleaf deciduous forest located in the south-eastern USA (mature oak), and a warm grassland located in the south mid-western USA. A summary of soil and key climatic and ecological conditions of the selected sites is given in Table 3.

3.2. Meteorological and flux data

Meteorological and eddy covariance flux data were collected at each site at a half-hourly time step, following Ameriflux research protocols (http://www.fluxnet.ornl.gov/fluxnet/). Instrumentation and data collection procedures are fully described in several publications, including Black et al. [9] and Amiro et al. [1] for the old aspen site (SOA), Humphreys et al. [34] for the Douglas-fir site (CR), Hansen et al. [33] for the temperate deciduous forest Walker branch watershed site (WBW), and Meyers [50] for the Little Washita warm grassland site (LW). Meteorological input variables to the stand-based versions of IBIS used here are incident shortwave and longwave radiation, mean air temperature, precipitation, relative humidity, wind speed, and barometric pressure. Where longwave radiation data were unavailable they were estimated using formulae of Brutsaert [11].

3.3. Root biomass data and estimates of RD and β for the modified IBIS simulations

The IBIS-mod simulations required estimates of root depth, *RD*, and of the β factor, which in turn depend upon measurements of root biomass density.

For the WBW site, only measurements of coarse root biomass were available (3.33 kg C m^{-2}; http://www.fluxnet.ornl.gov/fluxnet/). Total root biomass was therefore estimated assuming that fine root biomass represents 15% of total root biomass, based on a relationship established for Canadian boreal deciduous species [47]. The estimated total root biomass was then 3.92 kg m^{-2}, which yielded *RD* and β values of 0.82 m and 0.9658, respectively. This estimated *RD* (0.82 m) agrees very well with a previous estimate of 0.75 m reported by DeAngelis et al. [19], when the WBW forest was about 15 years younger.

For the SOA site, Steele et al. [59], using data collected during the BOREAS field campaign in 1994, reported that root biomass at that site was 2.78 kg C m^{-2}. Arora and Boer [4] proposed a

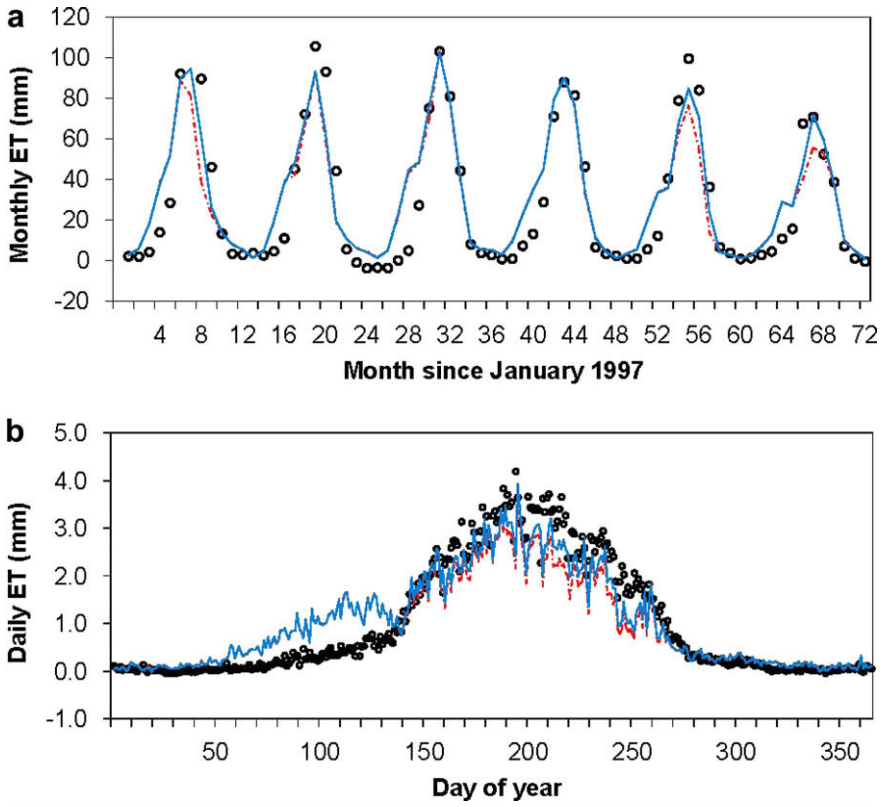

Fig. 5. Seasonal variation of simulated and measured ET at the SOA site. (a) Monthly variation; (b) average daily variation over the entire period of the simulations (1997–2002). Dots, dotted lines and solid lines refer to measured, standard and modified IBIS simulations, respectively.

unique value of C (Eq. (14)) for all boreal trees. The latter assumption is, however, highly speculative because both observations of Strong and La Roi [60], made in Canadian boreal forests, and the global map of root profile distribution of Jackson et al. [36] indicate a noticeable difference between root profiles of boreal deciduous and coniferous trees. Therefore, we used Strong and La Roi's [59] observations (rooting depth of about 1 m for boreal deciduous trees) to calculate β of about 0.9705 at the SOA site.

For the LW grassland site, no measurements of root biomass were available. Instead, we first estimated leaf biomass from leaf area index (LAI) assuming a specific leaf area (SLA) of 20 m^2 $(kg\ C)^{-1}$. We then assumed that root biomass of grasses represents about half of total plant biomass, to yield an estimate of 0.3 kg m^{-2}. Using the value of C for crops of 0.87 suggested by Arora and Boer [4], our calculations yielded 1.32 m for RD and 0.9775 for β. Our assumptions for SLA and root biomass are not unrealistic as they are similar to values used in several biophysical models, including IBIS. Observations of Schulze et al. [57] also suggest an SLA value (16.9 m^2 kg C^{-1}) for temperate grasses that is close to the 20 m^2 kg C^{-1} we used here.

For the Douglas-fir site, the reported mean total soil depth is 1 m to bedrock with no reported measurements of root biomass. We therefore used the same root profile in both IBIS-st and IBIS-mod simulations. Assuming that roots at that site are distributed over the entire soil profile (because the soil is shallow), β was estimated to be 0.905. The latter value was also used to parameterize IBIS-st because the Jackson et al.' [36] generic value used for temperate coniferous trees (0.982), applies to soils that are assumed to be more than 4 m deep.

4. Results

Our simulations were made using prescribed vegetation conditions. In particular, seasonal variations in LAI at the WBW and SOA deciduous forest sites were taken from observations described in Baldocchi et al. [6] and Barr et al. [7], respectively. This ensured that differences in the results obtained from IBIS-st and IBIS-mod simulations could be attributed entirely to differences in the representations of root water extraction and soil water stress, without the confounding effects of simulated phenology and other changes in vegetation state.

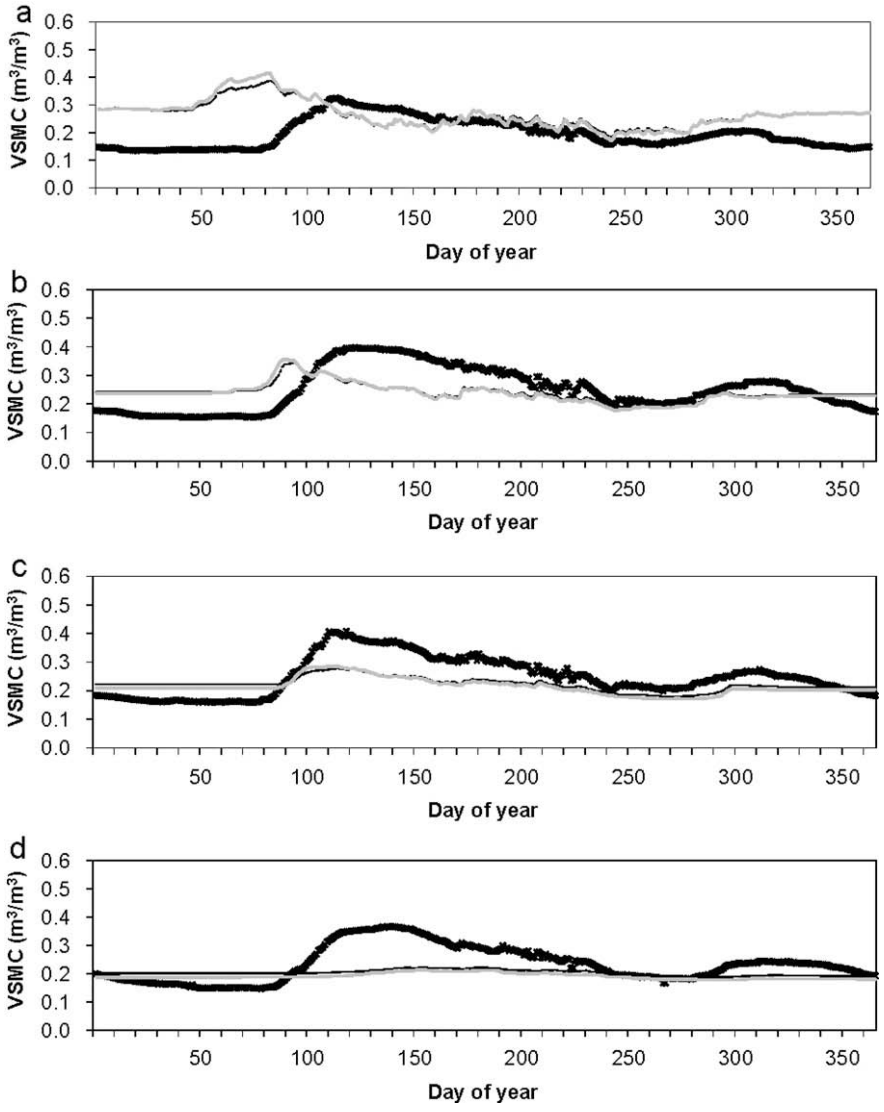

Fig. 6. Simulated and measured seasonal variation of volumetric soil moisture content (VSMC) at the SOA site. Shown are average daily variations over the entire period of the simulations (1997–2002). Crosses (Thickest dark line), thin solid line and thick gray solid line refer to measured, standard and modified IBIS simulations, respectively. (a) 0–10 cm; (b) 10–25 cm; (c) 25–50 cm; (d) 50–100 cm.

As a first step, it was important to assess how net radiation (R_n) was simulated by the two versions of the model at each site. This is because R_n is the main driver of ET, and hence largely determines partitioning of the water budget between ET and runoff. The agreement between measured and simulated data was fairly good (Fig. 2), with IBIS-mod producing generally better simulations of R_n than IBIS-st. At the LW site, the absolute mean bias error (MBE) reached ~18% for IBIS-st, but only ~3% for IBIS-mod (Table 4). The overall better simulation of R_n by IBIS-mod resulted from an overall better simulation of soil temperature.

4.1. Campbell River site (Douglas-fir forest)

At the Douglas-fir dominated CR site, the dynamic RWU scheme incorporated in IBIS-mod yielded improved simulations of daily ET during the relatively dry period in summer, when high atmospheric vapour pressure deficit was combined with low soil water availability (Fig. 3a and b). This caused greater simulated soil water depletion than obtained with IBIS-st (Fig. 4a–c). In fact, during relatively dry periods when soil moisture content is low, simulated water extraction is enhanced in IBIS-mod through the use of a higher λ value (Eq. (10)). The automatic adjustment of λ in IBIS-mod allows the plant to extract water preferentially from wetter layers first. The two models operate, however, similarly from October to April, when atmospheric demand for evaporation is low (Fig. 3a and b). The difference in model behavior between the two versions is also consistent for all years (Fig. 3a), which shows that dynamic RWU scheme should contribute a significant improvement to decadal or longer term simulations.

As water budget is mainly partitioned between Et, soil moisture and runoff (surface and subsurface), The underestimation of both daily ET and daily soil moisture by both versions of the model during the first and the last three months of the year is very likely due to an overestimation of surface runoff and/or drainage during that period, where the site location receives the greatest portion of annual precipitation (Figs. 3a and b and 4a–c). In summer, IBIS-st underestimated both ET and soil moisture whereas IBIS-mod overestimated ET, which is somewhat consistent with its underestimation of soil moisture. This suggests that the runoff simulation was more realistic in IBIS-mod than in IBIS-st during summertime. The simulated partitioning of water from precipitation into runoff in IBIS-mod, in winter, and in IBIS-st, all year round, is likely too high. This may result from difficulties in modeling vertical water movement in soils with high sand content. There are several other model imperfections that could also contribute to poor representation of annual runoff (and ET), in common with many LSMs applied to forest ecosystems. These include: biases due to numerical approximation (e.g., [15]); the use of soil vertical resolutions that are much coarser than required according to theoretical analysis in conjunction with use of Darcy's law (e.g., [20]), the overlook of lateral water flow and its effects on soil-surface hydrology [14,23,64]; imperfections in the definition of rooting depth and in the incorporation of nutrient limitations on root water uptake [37,69]; the overlook of stone content in the estimation of soil water holding capacity (stone fractions may exceed 30% in some regions of the world) (e.g., [8,39]); and the mis-consideration of the effects of mosses, lichens and litter layers on hydrological regimes [14,25,66].

Seasonal variation of simulated ET improved appreciably with IBIS-mod (r^2 between simulated and measured monthly rates were 0.84 and 0.96 for IBIS-st and IBIS-mod, respectively). On a yearly basis, average measured ET was 386 mm, with IBIS-st and IBIS-mod simulations estimating 326 mm (84%) and 360 mm (93%), respectively. These differences in simulated ET were entirely due

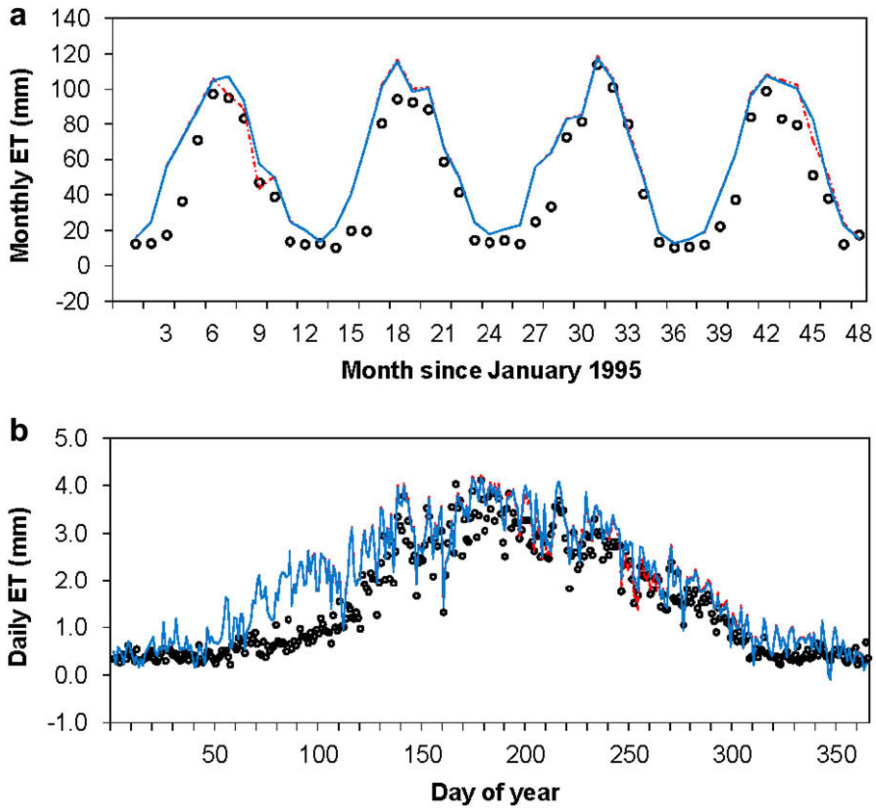

Fig. 7. Seasonal variation of simulated and measured ET at the WBW site. (a) Monthly variation; (b) average daily variation over the entire period of the simulations (1995–1998). Dots, dotted lines and solid lines refer to measured, standard and modified IBIS simulations, respectively. Measured data refer to the period 2002–2004.

to the difference between the two versions of IBIS in the representation of RWU as the simulations by both versions were based on identical assumptions about root distribution (Section 3.3). Further analyses on annual estimates of ET are given in Section 4.6.

4.2. BOREAS_SSA (old aspen forest)

At the SOA site IBIS-mod yielded better estimates of ET than IBIS-st during the summer (roughly, days 180 through 270; Fig. 5a and b). Between mid-winter and mid spring, however, both model versions overestimated ET, as a direct consequence of their overestimation of soil moisture (Figs. 5a and b and 6a–d). Based on results of a model intercomparison study in cold ecosystems [10,51], the overestimation of soil moisture in winter is very likely due to the underestimation of free drainage, while overestimation at the beginning of the growing season (roughly days 100–150) is likely caused by the model not adequately capturing the timing of snow melt and the interplay between runoff and soil water infiltration. These soil moisture simulations are very similar to those obtained by Ju et al. [38] using the BEPS model, which somewhat confirms the general difficulty of state of the art LSMs to capture accurately some cold ecosystem hydrological features.

Because the root profile is simulated differently in IBIS-st and IBIS-mod (see Section 3.3), we performed an additional simulation with IBIS-mod to separate the effect of the new RWU scheme (Section 2.2.2) from the effect of the new root profile (Section 2.2.2) on simulated ET in this boreal ecosystem. When only the new RWU was incorporated in IBIS-mod, simulated ET was less than 2% higher than that simulated by IBIS-st. This indicates that the new representation of root distribution within the soil profile in IBIS-mod was the main cause of the improvement in ET simulation between days 180 and 270 (Fig. 5a and b), i.e., because roots are able to extract water from deeper levels in the soil in IBIS-mod ($\beta = 0.9705$) than in IBIS-st ($\beta = 0.943$).

Seasonal variation in ET was also better simulated by IBIS-mod at SOA, as the regressions between simulated and measured

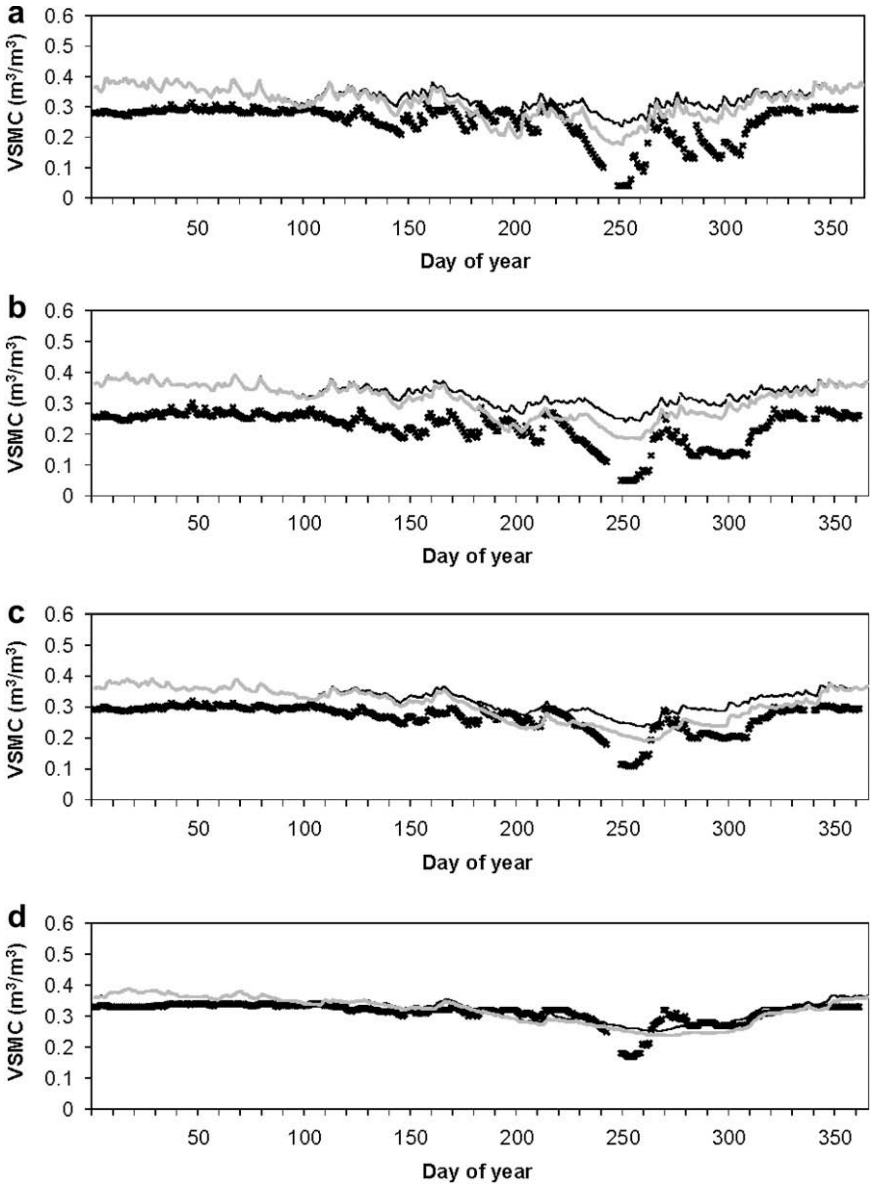

Fig. 8. Simulated and measured seasonal variation of volumetric soil moisture content (VSMC) at the WBW site. Shown are average daily variations over the entire period of the simulations (1995–1998). Crosses (thickest dark line), thin solid line and thick gray solid line refer to measured, standard and modified IBIS simulations, respectively. (a) 0–10 cm; (b) 10–25 cm; (c) 25–50 cm; (d) 50–100 cm. Measured data were collected between 2002 and 2004, and are plotted for illustration only.

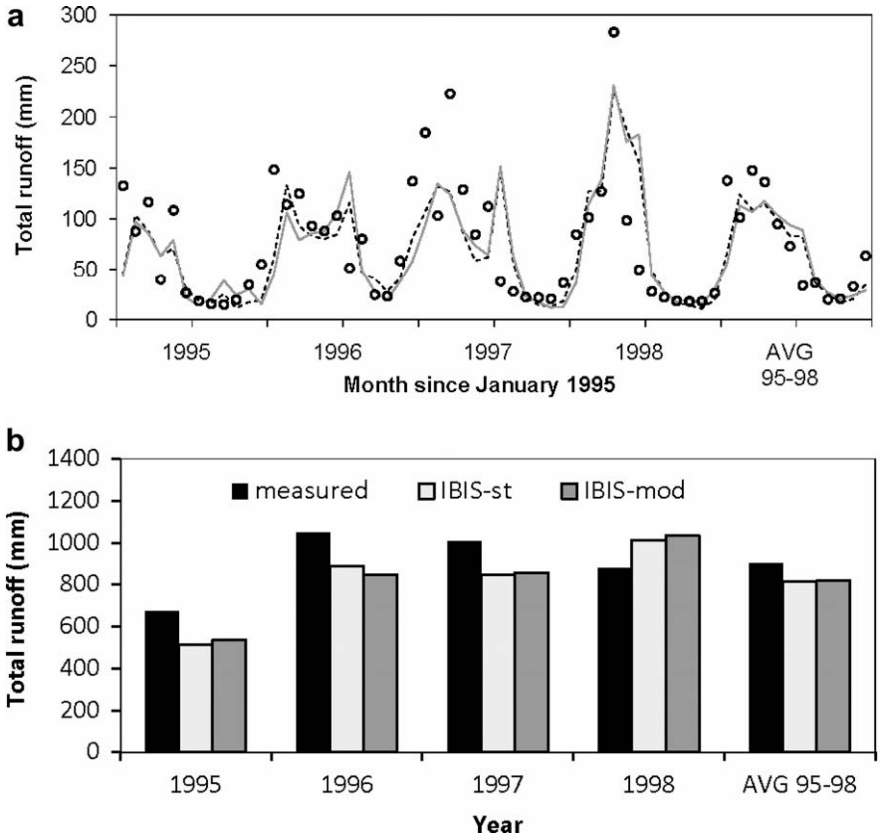

Fig. 9. Seasonal (a) and annual (b) variations simulated and measured runoff at the WBW site. Dots, dotted line and solid line refer to measured, standard and modified IBIS simulations, respectively. The quantities shown in (a) and (b) refer to the sum of soil surface and sub-surface (drainage) runoff components.

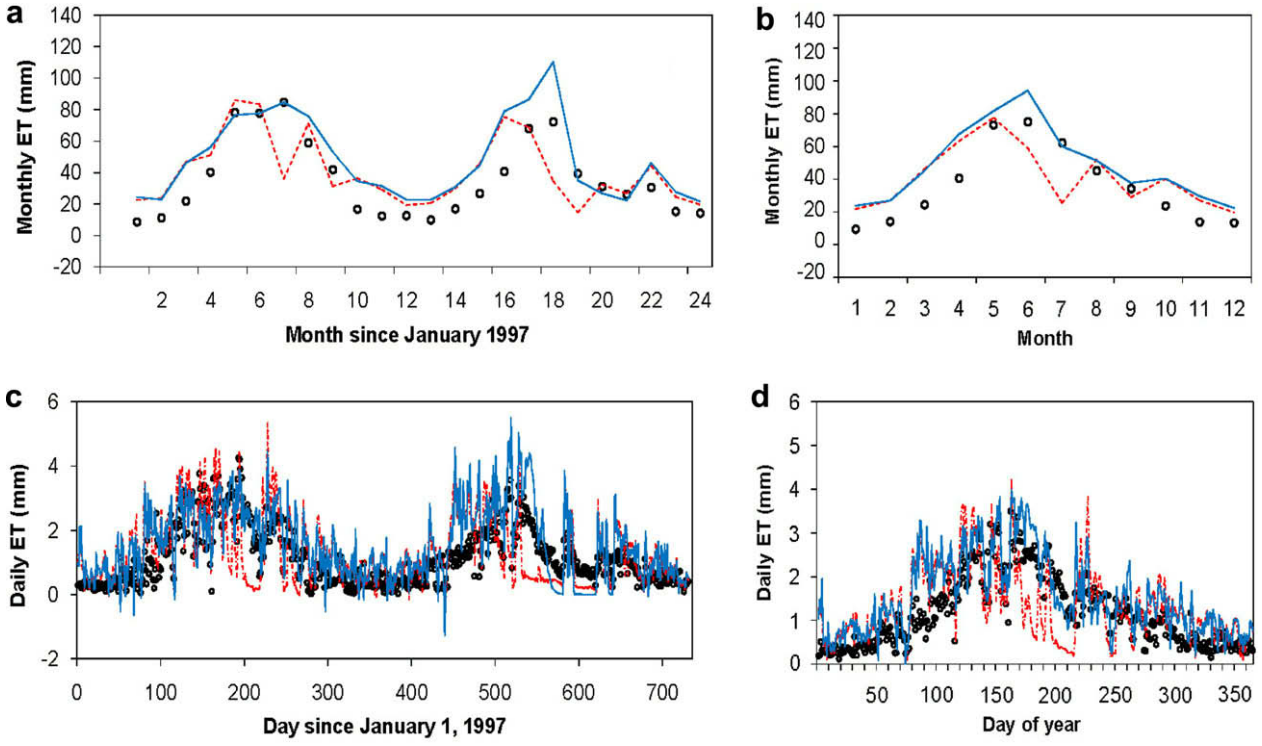

Fig. 10. Seasonal variation of simulated and measured ET at the LW site. (a) Monthly variation; (b) average monthly variation over the entire period of the simulations (1997–1998); (c) daily variation; (d) average daily variation over the entire period of the simulations (1997–1998). Here, simulated data over the entire period of simulations are shown, in addition to averages, to illustrate clearly the behavior of the two versions of the model under very low soil moisture conditions. Dots, dotted lines and solid lines refer to measured, standard and modified IBIS simulations, respectively.

monthly data yielded r^2 of 0.81 and 0.87 for IBIS-st and IBIS-mod, respectively. On a yearly basis, IBIS-mod estimated 384 mm total compared to 363 mm for IBIS-st and 359 mm measured (see Section 4.6 for more analyses of these annual estimations).

4.3. Walker branch watershed site (oak forest)

This temperate forest site receives an adequate moisture supply from precipitation almost year round, and hence predicted ET was generally very similar between the two versions of IBIS. They diverged slightly during the relatively dry El Niño summers of 1995 and 1998 (Fig. 7a and b). The very slight difference (~1%) in simulated annual ET for the comparatively wet years 1996 and 1997 confirms that the static and the dynamic RWU schemes used in IBIS-st and IBIS-mod, respectively, were operating in a similar manner under well-watered conditions (see Eqs. (5) and (9) in IBIS-st and Eqs. (10) and (11) in IBIS-mod, and the analytical explanation in Section 4.4). Comparison of simulated average daily soil moisture data by the two models indicates a larger depletion of soil water in IBIS-mod (Fig. 8a–d), which resulted from a larger simulated ET during the 1995 and 1998 summer periods.

For both simulations, a correlation of 0.9 was obtained between simulated and measured monthly ET. Both model versions dampened the seasonal variation of ET as the monthly data analyses revealed a coefficient of variation (CV) 20% lower for the simulated data (0.58) than for the measured data (0.73). Average annual values indicate a 27% and a 28% overestimation of ET by IBIS-st and IBIS-mod, respectively, which will be discussed further in Section 4.6.

As runoff is an important term of the water budget, it is interesting to examine the performance of IBIS when both static and dynamic RWU schemes are implemented. Comparison between measured and simulated data suggest good runoff simulation by both versions at this site (Fig. 9a and b). Annual averages indicate that the departure between measured (900 mm) and simulated runoff by both IBIS-st (814 mm) and IBIS-mod (818 mm) versions is less than 10%.

Measurements of runoff refer to the sum of surface and sub-surface (drainage) runoff components. Measured runoff quantities were obtained by summing the measured discharge at the east and the west catchments of the WBW and dividing the obtained sum by the total watershed area (97.5 ha), as described in Luxmoore and Huff [49] and Wilson et al. [68].

4.4. Little Washita site (warm grasses)

The LW site was subjected to a severe drought during the summer of 1998 [51], which offered a unique opportunity to compare IBIS-st and IBIS-mod performances under extremely dry conditions, as opposed to the wet conditions of the WBW site. The

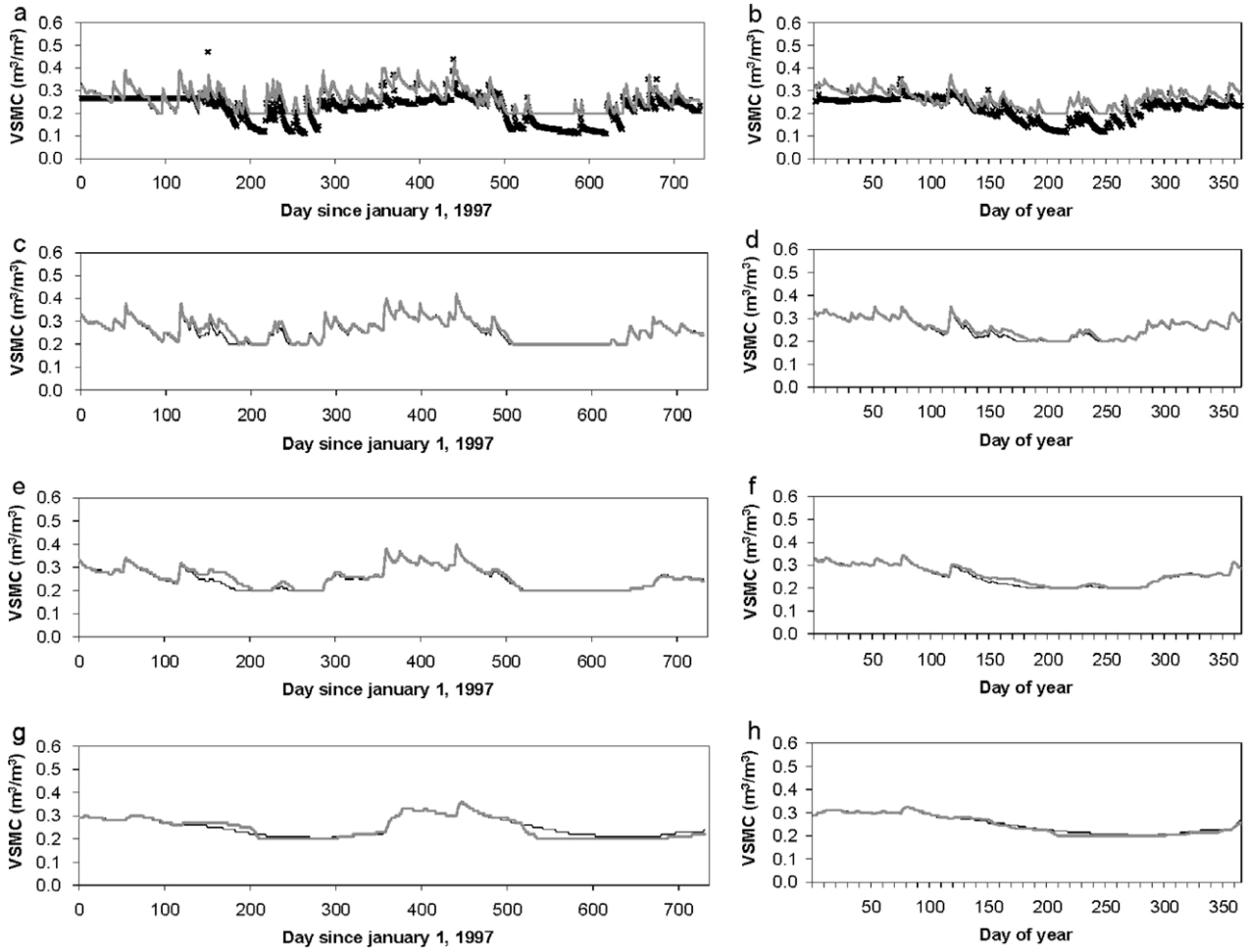

Fig. 11. Simulated and measured daily (a, c, e and g panels) and average daily (b, d, f and h panels) variation of volumetric soil moisture content (VSMC) at the LW site, over the entire period of the simulations (1997–1998). The results are shown for the 0–10 cm soil layer (a) and (b); the 10–25 cm soil layer (c) and (d); the 25–50 cm soil layer (e) and (f); and for the 50–100 cm soil layer (g) and (h). These four soil layers correspond to the soil vertical profile where more than 97% of roots are found. Crosses (thickest dark line), thin dark solid line and thick gray solid line refer to measured, standard and modified IBIS simulations, respectively.

1998 drought is demonstrated in measured soil moisture dropping to very low levels, even below the theoretical wilting point threshold of the clay loam soil found at LW [$\sim$0.197 m^3 m^{-3}] (Fig. 11a).

When soil moisture content is very low, IBIS-mod simulates the variation of ET more realistically than IBIS-st, as seen in Figs. 11a–d and 11a–h for days 150–250 (1997), and days 500–600 (1998). The greater use of soil water and larger response to the atmospheric demand for evaporation by IBIS-mod, under low soil water conditions, is explained by the forms of Eqs. (5) and (9) (IBIS-st), compared to Eqs. (10) and (11) (IBIS-mod). When soil moisture is low, the numerator in Eq. (5) tends towards zero as the exponential term tends towards 1, causing the simulated water stress term in IBIS-st (Eq. (9)) to be very low (where a low value indicates high water stress). This causes a strong inhibition of plant transpiration, and hence of ET (soil evaporation under dry soil conditions is also very low). In IBIS-mod, the effect of soil water stress on transpiration at low soil moisture conditions is moderated because of the continual orientation of roots towards extraction of water from wetter soil layers first (Eq. (10) and Table 1), associated with the enhanced capacity to extract water from the soil (Eq. (12) and Fig. 1).

As the soil dries out, transpiration tends to become the only mechanism by which water is removed from the soil. Transpiration is almost completely inhibited when soil moisture in all root layers reaches wilting point, which should prevent soil moisture from ever dropping below this level, as seen for both model versions around day 600 in Fig. 10c and Fig. 11a, c, e and g. Complete inhibition of plant water uptake at wilting point, is a common feature in several LSMs including, for example, BEPS [48], MOSES [27] and CLASS-TEM [3].

On a seasonal basis, at LW site, the correlations between measured and simulated ET were 0.50 and 0.82 for IBIS-st and IBIS-mod, respectively, with CVs indicating a 14% and 11% dampening of the seasonal variability, respectively. On an annual basis, the models overestimated average measured ET (429 mm) by 14% and 35%, respectively. Section 4.6 provides analyses of the annual estimates of ET.

4.5. Sensitivity analyses

As the representation of RWU is the main difference between IBIS-st and IBIS-mod, it is important to examine how the magnitude of the difference between simulated ET by the two versions of the model compares with the magnitude of the effect that uncertainties in some key soil parameters may have on simulated ET. Furthermore, water drainage out of the bottom of the soil system is controlled in IBIS by a soil permeability parameter (BPERM). This important parameter varies between 0 for impermeable soils and 1 for fully permeable soils, and may play an important role on simulated water budget. Because field estimates of BPERM are very rarely available, IBIS assigns a standard best guess value (0.1) for it, which has been used in our simulations. It is, therefore, also important to compare the magnitude of the difference between simulated ET by IBIS-st and IBIS-mod with the magnitude of the effect that uncertainties in BPERM may have on ET simulations.

Sensitivity of ET as simulated by IBIS-st to ±20% changes in saturated hydraulic conductivity (SHC), air-entry potential (AEP; saturated matric potential) and *b*-power of moisture release (MRP; Eq. (12)), as well as to changes in BPERM was carried out and compared to IBIS-mod simulations, as shown in Fig. 12 and Table 5.

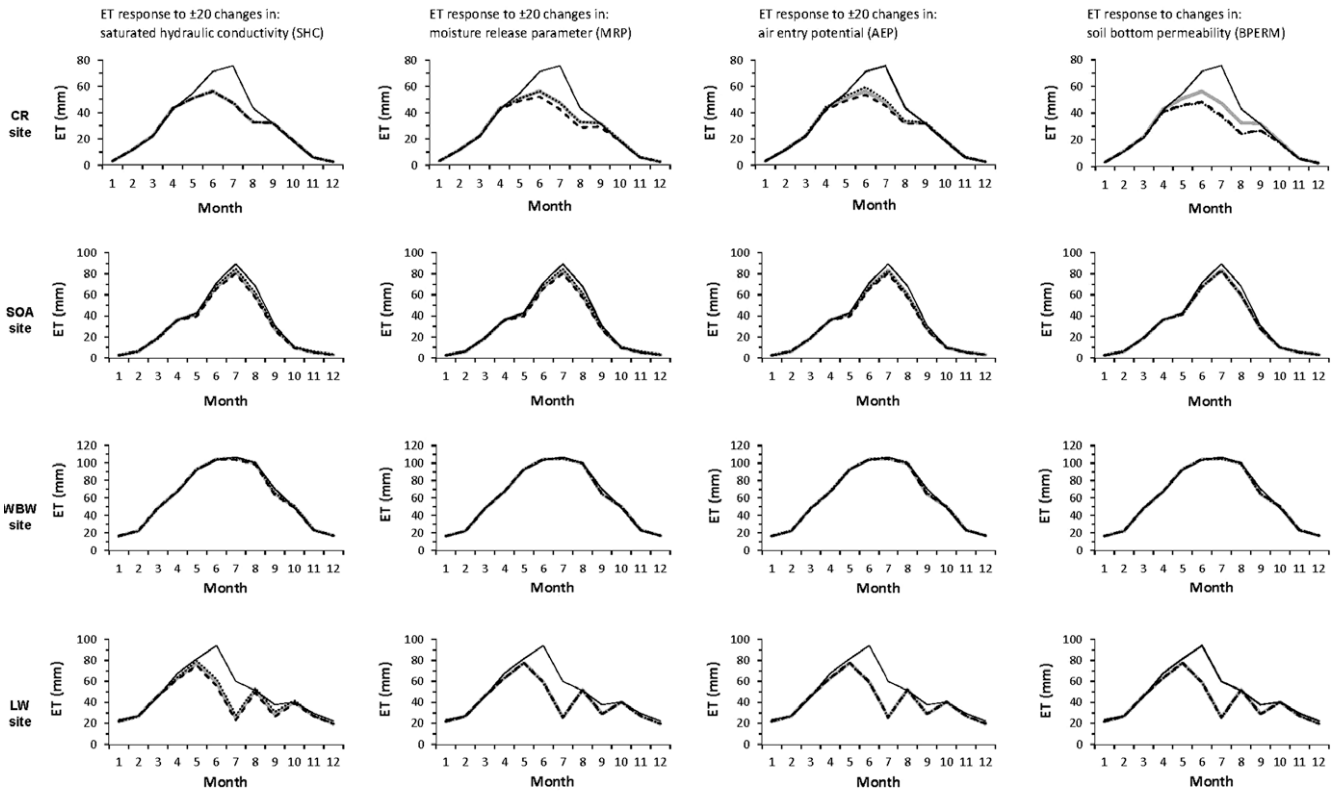

Fig. 12. Average monthly variation of ET as simulated by IBIS-st (thick solid line) and IBIS-mod (thin dark solid line). Also shown, results of IBIS-st simulations when soil saturated hydraulic conductivity (SHC), the moisture release parameter (MRP; *b* in Eq. (12)) and the air entry potential (AEP) were perturbed by ±20%, and when BPERM parameter was increased from its standard value (0.1) to 0.5 and 0.9. Numbers between brackets show the departure (in mm) from IBIS-st simulation. Dashed and dotted lines refer to IBIS-st simulations when a given parameter is decreased and increased by 20%, respectively; and when BPERM value is increased to 0.5 and 0.9, respectively.

Table 5
Average annual simulated values of ET (mm) as simulated with IBIS-st and IBIS-mod. Also shown, results of IBIS-st simulations when soil saturated hydraulic conductivity (SHC), the moisture release parameter (MRP; b in Eq. (12)) and the air entry potential (AEP) were perturbed by ±20%, and when the soil permeability parameter (BPERM; see text) was increased from its standard value, 0.1 to 0.5 and 0.9. Numbers between brackets show departure (in mm) from IBIS-st simulation.

	IBIS-st	IBIS-st with changes in SHC		IBIS-st with changes in MRP		IBIS-st with changes in AEP		IBIS-st with changes in BPERM		IBIS-mod
		−20%	+20%	−20%	+20%	−20%	+20%	0.5	0.9	
CR	326	326 (0)	326 (0)	306 (−20)	326 (0)	315 (−11)	335 (9)	288 (−37)	285 (−41)	380 (54)
SOA	363	359 (−4)	365 (2)	362 (−1)	363 (0)	362 (−1)	363 (0)	362 (−1)	362 (−1)	384 (21)
WBW	711	706 (−5)	713 (−2)	711 (0)	712 (0)	707 (−4)	716 (5)	711 (0)	710 (−1)	714 (3)
LW	487	470 (−17)	501 (14)	487 (0)	487 (0)	488 (1)	486 (−1)	487 (0)	487 (0)	579 (92)
Average	472	465 (−6)	476 (4)	467 (−5)	472 (0)	468 (−3)	475 (3)	462 (−9)	461 (−10)	514 (43)

The results show that the new representation of RWU in IBIS has a larger effect that what ±20% uncertainty in soil parameters might have on ET simulations at CR, SOA and LW sites (Fig. 12 and Table 5). This is, especially during periods of high atmospheric demand for evaporation and low precipitation, as during summer at CR and LW sites (Fig. 12). At the very wet site of this study, WBW, where the static and the dynamic RWU schemes must yield very similar results (see Sections 4.3 and 4.4), the imposed changes in soil parameters caused changes in ET that are comparable to those caused by the implementation of the new RWU scheme (Fig. 12 and Table 5). On an annual basis, the average difference between IBIS-st' simulated ET and IBIS-mod' simulated ET reached 43 mm while ET changes due to ±20% perturbations in SHC, AEP and MRP and due to increased BPERM from 0.1 to 0.9 did not exceeded an average of 6 mm (Table 5). For the driest site (LW), the difference between IBIS-st and IBIS-mod simulations of ET reached 92 mm while the most important changes in ET that have been caused by changes in soil parameters reached only 17 mm (Table 5).

4.6. Summary of obtained results at all sites

Grouping monthly ET data for all sites (Fig. 13a–c), shows that the correlation between simulated and measured data is better for IBIS-mod ($r^2 = 0.83$) than for IBIS-st ($r^2 = 0.76$) – indicating that the dynamic RWU scheme combined with the new representation of rooting depth brought a general improvement across a range of contrasting ecosystems. This was further confirmed by results of the statistical t-test of significance. The two-tailed Student's t-test (p) yielded indeed probability (p) values of 0.13 and 0.00 for IBIS-st and IBIS-mod, respectively. Note that a p of 0.05 or lower indicates a departure from the observation that is significant at the 95% confidence level.

Monthly averages of measured ET, and those simulated by IBIS-st and IBIS-mod at all sites were 35.7 mm (CV = 0.83), 36.7 mm (CV = 0.78) and 39.3 mm (CV = 0.77), respectively. However, the measured ET is very likely an underestimate because of problems with energy balance closure, a common feature of eddy covariance measurements [61,67]. Measured energy flux data at the four sites indicate, indeed, the existence of annual energy imbalances (computed from sensible (H) and latent (λE) heat terms, and from net radiation (R_n) and soil heat flux (G) as $[1 - (H + \lambda E)/(R_n + G)]$) that average 30%, 22%, 26%, and 30% at CR, WBW, SOA and LW, respectively. Such important energy imbalances are indicative of important inaccuracies and uncertainties in measured ET, which could significantly bias our analyses on the performance of IBIS-mod relatively to IBIS-st. It is, therefore, worthwhile providing an estima-

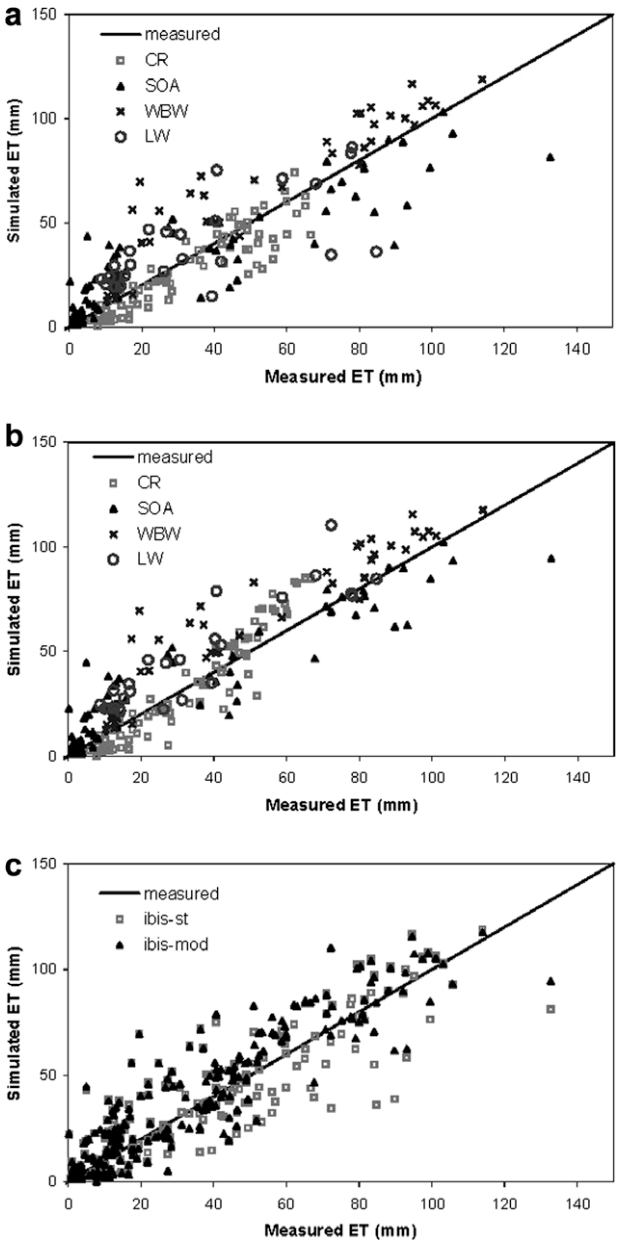

Fig. 13. Simulated *versus* measured average monthly ET at all sites. (a) Standard IBIS; (b) modified IBIS; (c) all standard and modified simulations compared.

tion of the magnitude of uncertainties in measured ET in order to strengthen our evaluation of the dynamic RWU *versus* the static one.

To estimate the magnitude of error in measured ET at each site, we attempted to close the measured energy budget. This is fundamentally important as an unclosed energy budget represents a violation of the energy conservation principle. Our approach to close the energy budget used the Bowen ratio (BR) method as described in Twine et al. [61], assuming that measurements of net radiation are generally accurate as it is generally well accepted among land surface scientists [61,67]. This means that the imbalance in energy budget is due to underestimation of measured λE, H or both. The close up of energy budget using the BR method yields new estimates of measured ET (termed, thereafter, corrected ET) that are 114 mm higher in average than EC measurements estimates, as shown in Table 6. Overall, the corrected estimates of ET suggest that IBIS-mod yield more accurate simulations of ET than IBIS-st, particularly under the dry conditions of the LW site (Table 6).

Table 6
Average annual measured and simulated ET (mm) at all sites. Numbers between brackets indicate the relative departure from corrected measured ET.

	Measured	Measured with correction	IBIS-st	IBIS-mod
CR	386	447	326 (−27%)	380 (−15%)
SOA	359	460	363 (−21%)	384 (−17%)
WBW	577	713	711 (<1%)	714 (<1%)
LW	429	569	487 (−14%)	579 (+2%)
Average	433	547	472 (−14%)	514 (−6%)

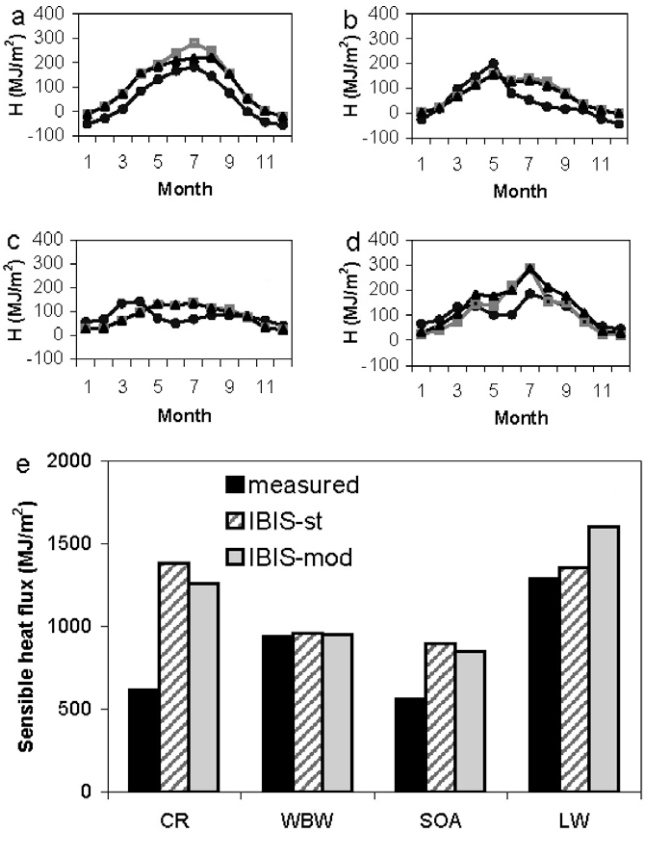

Fig. 14. Simulated and measured average seasonal variation of sensible heat flux at: (a) CR site; (b) SOA site; (c) WBW site; (d) LW site. Fluxes in (a)–(d) correspond to monthly totals while total annual fluxes are shown in (e).

Furthermore, the departure between simulated annual ET and corrected measured ET at all sites averaged a much lower rate for IBIS-mod (6%) than for IBIS-st (14%) (Table 6).

Because net radiation is partitioned primarily into λE and H at vegetated sites, it is worth briefly examining results of H simulations. Except for the LW site, as shown in Fig. 14a–e, IBIS-mod predicts lower H both in summer and year-round than does IBIS-st, as would be expected given the generally higher λE simulated by IBIS-mod. The LW site differs from this general pattern because it is dominated by grasses, with soil heat flux forming a larger component of the energy balance. Soil heat flux simulated by IBIS-st was about 20% higher than in IBIS-mod – which caused both H and λE in IBIS-mod to exceed those in IBIS-st.

Fig. 15a and b illustrate the effect of the static and the dynamic RWU approaches on the vertical soil moisture profile for WBW and LW sites, respectively. It is shown that for the WBW site, which is a humid ecosystem, the dynamic approach cause more extraction of water from the soil during the entire growing season period (∼ between days 100 and 300), but that extraction is more oriented towards the three top soil layers (Fig. 15a). Presumably, because of frequent rainfall conditions at the WBW site that causes top soil layers to be almost always wet. Conversely, for the LW dry site, soil water extraction from bottom layers become more and more important as conditions become more and more dried (Fig. 15b).

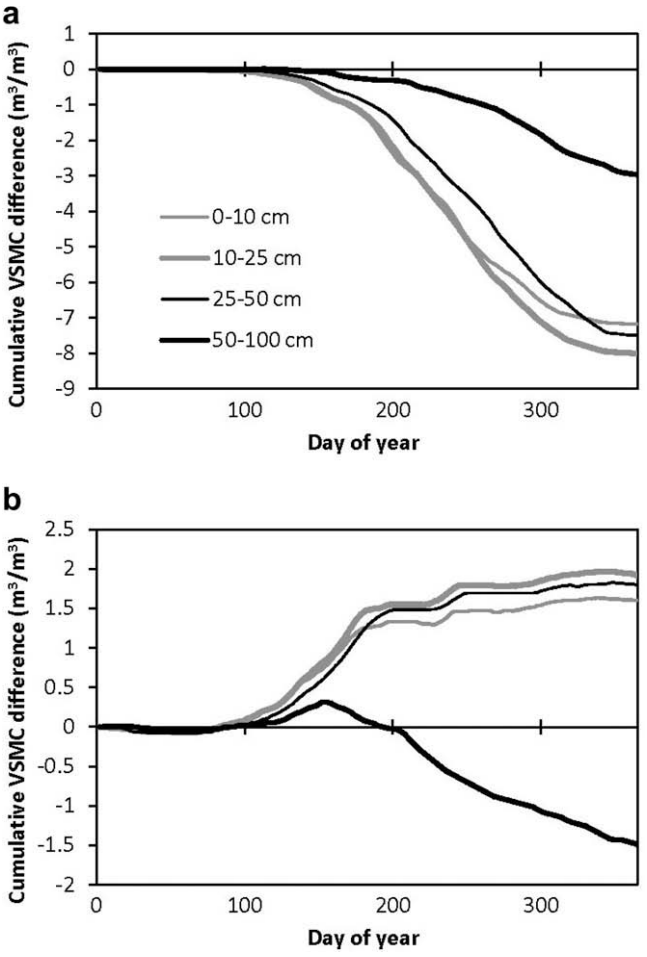

Fig. 15. Effects of the static and the dynamic RWU approaches on average soil moisture profile throughout the year, at WBW site (a) and LW site (b). The *y*-axis shows the cumulative volumetric soil moisture content (VSMC) difference between IBIS-mod and IBIS-st.

5. Concluding discussion

The representation of the effects of water stress on the response of stomatal conductance to soil water deficits and hence on mass exchanges (CO_2 and water vapour) between plants and the atmosphere is a critical issue in the field of land surface modeling [21,29,55]. As LSMs are increasingly used to tackle a variety of scientific and management questions, there have been recent warnings about the need for adequate representations of plant water uptake [37,38,45,55]. The main objective of this study was to compare two RWU schemes on 1-dimensional hydrological simulations in a widely used LSM, IBIS. The first scheme is the standard algorithm used in published IBIS studies, while the second combines a slightly modified RWU scheme recently proposed by Li et al. [45] with new calculations of root distribution (from root biomass) suggested by Arora and Boer [4]. The standard RWU scheme is classified as *static* because the extraction of water from a given soil layer depends exclusively upon the proportion of plant roots in that soil layer. The modified IBIS incorporates a RWU scheme, classified as dynamic, because the amount of water extracted by roots from a given soil layer depends on its water content and the density of plant roots, as well as on the water contents of adjacent layers. Extraction of water in the dynamic scheme is continuously adjusted in such a way that water is extracted preferentially from the wetter layers. Consequently, this dynamic representation of RWU in the model captures a natural tendency of plants to optimize their energy expenditures when extracting water from the soil, in agreement with field observations (e.g., [32,40]).

The results indicate that under relatively well watered conditions, such as those found at the temperate deciduous WBW site, the two RWU schemes produce very similar simulations of ET, though soil water extraction and ET were generally greater with the dynamic RWU scheme, notably in a relatively dry year (1995). This suggests that when LSMs are used to simulate water budget of wet vegetated ecosystems, it is perhaps preferable to use the RWU scheme that is the less costly in terms of computational time, namely the static one. With drier site conditions, as generally occurs during summer at the west coastal CR site, differences between simulations with the static and the dynamic RWU schemes become more evident, with the latter extracting more water to meet evaporative demand. Furthermore, results for the SOA site highlight the importance of taking root dynamics effects into account when simulating water budget components in LSMs.

Overall, our results indicate a better use of soil water to meet simulated evaporative demand, when the dynamic RWU scheme is implemented. This inference is supported by a general improvement in correlations between simulated and measured ET. However, the most striking differences in ET simulations were obtained at the grassland LW site, where very dry conditions are common. Under such conditions, the dynamic RWU scheme yielded a much more realistic use of the available soil water by the vegetation and, hence, to better agreement between model estimates and observed data of ET. This suggests that the dynamic RWU scheme, in contrast to the static scheme, was able to mimic the crucial physiological process by which C_4 plants survive severe droughts. Given that many GCM projections of future climate indicate more frequent and/or more intense drought events occurring in some regions of the globe [35], better representations of vegetation responses to drought are needed in LSMs. The use of dynamic RWU schemes such as the one developed and tested here may help with this objective. Our analyses also showed that proper validation of LSM simulations of heat and mass exchanges between the land surface and the atmosphere ideally requires a rigorous procedure for correcting imbalances in the measured canopy energy budget. In this study, we used the Bowen Ratio method to close the energy budget of measured data, as it has been recommended by Twine et al. [61]. According to our current knowledge of ecosystem processes, a more appropriate approach to close the energy budget would be one that considers the coupling among carbon and energy flows, which does not exist yet [24].

Acknowledgements

This study is part of the Fluxnet Canada Research Network modeling activities supported by the Natural Science and Engineering Council of Canada and the Canadian Foundation of Climate and Atmospheric Sciences. Funding was provided in part under the Natural Resources Canada Panel on Energy Resources Development P.O.L. 6.2.1, Enhanced Greenhouse Gas Sinks program. We thank Fluxnet-Canada and Ameriflux researchers for making eddy covariance data and supporting meteorological data accessible, including specifically: D. Baldocchi, A. Barr, T.A. Black and T. Meyers. We thank Dr. Kaiyuan Li from University of Washington for insightful discussions during the preparation of this manuscript. We are grateful to four anonymous reviewers whose comments helped to substantially improve this manuscript.

References

[1] Amiro BD, Barr AG, Black TA, Iwashita H, Kljun N, McCaughey JH, et al. Carbon energy and water fluxes at mature and disturbed forest sites Saskatchewan Canada. Agr Forest Meteorol 2006;136:237–51.
[2] Arora VK. Modelling vegetation as a dynamic component in soil-vegetation-atmosphere-transfer schemes and hydrological models. Rev Geophys 2002;40:1006. doi:10.1029/2001RG000103.
[3] Arora VK. Simulating energy and carbon fluxes over winter wheat using coupled land surface and terrestrial ecosystem models. Agr Forest Meteorol 2003;118(1–2):21–47.
[4] Arora VK, Boer GJ. A representation of variable root distribution in dynamic vegetation models. Earth Interactions 2003;7 [Paper 6, 19pp.].
[5] Ashton PJ. Avoiding conflicts over Africa's water resources. Ambio 2002;31:236–42.
[6] Baldocchi DD, Falge E, Wilson K. A spectral analysis of biosphere–atmosphere trace gas flux densities and meteorological variables across hour to year time scales. Agr Forest Meteorol 2001;107:1–27.
[7] Barr AG, Black TA, Hogg EH, Kljun N, Morgenstern K, Nesic Z. Inter-annual variability in the leaf area index of a boreal aspen-hazelnut forest in relation to net ecosystem production. Agr Forest Meteorol 2004;126:237–55.
[8] Batjes NH. Development of a world data set of soil water retention properties using pedotransfer rules. Geoderma 1996;71:31–52.
[9] Black TA, den Hartog G, Neumann HH, Blanken PD, Yang PC, Russell C, et al. Annual cycles of water vapour and carbon dioxide fluxes in and above a boreal aspen forest. Glob Ch Biology 1996;2:219–29.
[10] Bowling LC, Lettenmaier DP, Nijssen B, Graham LP, Clark DB, El Maayar M, et al. Simulation of high latitude hydrological processes in the Torne–Kalix basin, PILPS phase 2e, 1: experiment description and summary intercomparisons. Global Planet Change 2002;38(1–2):1–30. 2003.
[11] Brutsaert W. In: Reidel D, editor. Evaporation into the atmosphere. Norwell, Masson; 1982.
[12] Campbell GS, Norman JM. An introduction to environmental biophysics. 2nd ed. Springer; 1998.
[13] Canadell J, Jackson RB, Ehleringer JR, Mooney HA, Sala OE, Schulze E-D. Maximum rooting depth for vegetation types at the global scale. Oecologia 1996;108:583–95.
[14] Chen JM, Chen X, Ju W, Geng X. A remote sensing-driven distributed hydrological model: mapping evapotranspiration in a forested watershed. J Hydrol 2005;305:15–39.
[15] Chen T, Henderson-Sellers A, Milly P, Pitman A, Beljaars A, Abramopoulos F, et al. Cabauw experimental results from the project for intercomparison of landsurface parameterisation schemes (PILPS). J Climate 1997;10:1194–215.
[16] Coe MT, Foley JA. Human and natural impacts on the water resources of the Lake Chad basin. J Geophys Res 2001;106:3349–56.
[17] Coe MT, Costa MH, Botta A, Birkett C. Long-term simulations of discharge and floods in the Amazon Basin. J Geophys Res 2002;107. 53-1 a 53-17.
[18] Costa MH, Oliveira CHC, Andrade RG, Bustamante TR, Silva FAA, Coe MT. A macroscale hydrological data set of river flow routing parameters for the Amazon Basin. J Geophys Res 2002;107. 44-1 a 44-9.
[19] DeAngelis DL, Gardner RH, Shugart HH. Productivity of forest ecosystems studied during the IBP: the woodlands data set. In: Reichle DE, editor. Dynamics of forest ecosystems IBP 23. Cambridge, UK: Cambridge University Press; 1981. p. 567–672.
[20] de Rosnay P, Bruen M, Polcher J. Sensitivity of the surface fluxes to the number of layers in the soil model used in GCMs. Geophys Res Lett 2000;27:3329–32.

[21] de Rosnay P, Polcher J. Modeling root water uptake in a complex land surface scheme coupled to a GCM. Hydr Earth Syst Sci 1998;2:239–56.
[22] Donner SD, Coe MT, Lenters JD, Twine TE, Foley JA. Modeling the impact of hydrological changes on nitrate transport in the Mississippi River Basin from 1955 to 1994. Glob Biogeoch Cycles 2002; doi:10.1029/2001GB001396.
[23] El Maayar M, Chen JM. Spatial scaling of evapotranspiration as affected by heterogeneities in vegetation, topography, and soil texture. Remote Sens Environ 2006;102:33–51.
[24] El Maayar M, Price DT, Chen JM. On the use of field measurements of energy fluxes to evaluate land surface models. Ecol Model 2008;214:293–304.
[25] El Maayar M, Price DT, Delire CD, Foley JA, Black TA, Bessemoulin B. Validation of the integrated biosphere simulator over Canadian deciduous and coniferous boreal forest stands. J Geophys Res 2001;106:14339–55.
[26] Entekhabi D, Asrar GR, Betts AK, Beven KJ, Bras RL, Duffy CJ, et al. An agenda for land-surface hydrology research and a call for the second international hydrological decade. Bull Amer Meteorol Soc 1999;80(10):2043–58.
[27] Essery RLH, Best MJ, Cox PM. MOSES 2.2 technical documentation. Hadley centre technical note 30, Met Office, Bracknell; 2001. <http://www.metoffice.gov.uk/research/hadleycentre/pubs/HCTN/HCTN_30.pdf>.
[28] Feddes RA, Hoff H, Bruen M, Dawson TE, de Rosnay P, Dyrmeyer P, et al. Modeling root water uptake in hydrological and climate models. Bull Amer Met Soc 2001;82(12):2797–810.
[29] Federer CA, Vorosmarty C, Fekete B. Sensitivity of annual evaporation to soil and root properties in two models of contrasting complexity. J Hydromet 2003;4:1276–89.
[30] Foley JA, Prentice IC, Ramankutty N, Levis S, Pollard D, Sitch S, et al. An integrated biosphere model of land surface processes, terrestrial carbon balance, and vegetation dynamics. Glob Biogeochem Cycles 1996;10(4):603–28.
[31] Gale MR, Grigel DF. Vertical root distributions of northern tree species in relation to successional status. Can J Forest Res 1987;17:829–34.
[32] Gardner WR. Soil properties and efficient water use: an overview. In: Taylor HM, Jordan WR, Sinclair TR, editors. Limitation to efficient water use in crop production. American Society of Agronomy; 1983. p. 45–6.
[33] Hanson PJ, Amthor JS, Wullschleger SD, Wilson KB, Grant RF, Hartley A, et al. Oak forest carbon and water simulations: model intercomparisons and evaluations against independent data. Ecol Monographs 2004;74:443–89.
[34] Humphreys ER, Black TA, Ethier GJ, Drewitt GB, Spittlehouse DL, Jork E-M, et al. Annual and seasonal variability of sensible and latent heat fluxes above a coastal Douglas-fir forest, British Columbia, Canada. Agr Forest Meteorol 2003;115:109–25.
[35] Intergovernmental Panel on Climate Change (IPCC). The science of climate change 2001, the scientific basis. Cambridge University Press; 2001.
[36] Jackson RB, Canadell J, Ehleringer JR, Mooney HA, Sala OE, Schulze ED. A global analysis of root distributions for terrestrial biomes. Oecologia 1996;108:389–411.
[37] Jackson RB, Schenk HJ, Jobbagy EG, Canadell J, Colello GD, Dickinson RE, et al. Belowground consequences of vegetation change and their treatment in models. Ecol Appl 2000;10:470–83.
[38] Ju W, Chen JM, Black TA, Barr AG, Liu J, Chen B. Modelling multi-year coupled carbon and water fluxes in a boreal aspen forest. Agr Forest Meteorol 2006;140:136–51.
[39] Kern JS. Geographic patterns of soil-water holding capacity in the contiguous United States. Soil Sci Soc Amer J 1995;59:1126–33.
[40] Kljun N, Black TA, Griffis TJ, Barr AG, Gaumont-Guay D, Morgenstern K, et al. Net carbon exchange of three boreal forests during a drought. In: Proceedings of the 26th conference on agricultural and forest meteorology, August 23–27, Vancouver, BC, Canada; 2004. p. 12.5.
[41] Koster RD, Milly PCD. The interplay between transpiration and runoff formulations in land surface schemes used with atmospheric models. J Climate 1997;10:1578–91.
[42] Kucharik CJ, Foley JA, Delire C, Fisher VA, Coe MT, Lenters J, et al. Testing the performance of a dynamic global ecosystem model: water balance, carbon balance and vegetation structure. Glob Biogeochem Cycles 2000;14(3):795–825.
[43] Laevesley GH. Modelling the effects of climate change on water resources – a review. Clim Change 1994;28:159–77.
[44] Legesse D, Vallet-Coulomb C, Gasse F. Hydrological response of a catchment to climate and land use changes in Tropical Africa: case study South central Ethiopia. J Hydrol 2003;275:67–85.
[45] Li KY, Coe MT, Ramankutty N. Investigation of hydrological variability in West Africa using land surface models. J Climate 2005;18:3173–88.
[46] Li KY, De Jong R, Boisvert JB. An exponential root-water-uptake model with water stress compensation. J Hydrol 2001;252:189–204.
[47] Li Z, Kurz WA, Apps MJ, Beukema SJ. Belowground biomass dynamics in the carbon budget model of the Canadian forest sector: recent improvements and implications for the estimation of NPP and NEP. Can J Forest Res 2003;33:126–36.
[48] Liu J, Chen JM, Cihlar J, Park W. A process-based Boreal ecosystems productivity simulator using remote sensing inputs. Remote Sens Environ 1997;62:158–75.
[49] Luxmoore RJ, Huff DD. 1989. Water. In: Johnson DW, Van Hook RI, editors. Analysis of biogeochemical cycling processes in walker branch watershed; 1989. p. 164–96
[50] Meyers TP. A comparison of summertime water and CO_2 fluxes over rangeland for well watered and drought conditions. Agr Forest Meteorol 2001;106:205–14.
[51] Nijssen N, Bowling LC, Lettenmaier DP, Clark DB, El Maayar M, Essery R, et al. Simulation of high latitude hydrological processes in the Torne–Kalix basin: PILPS phase 2(e) 2: comparison of model results with observations. Glob Planet Change 2003;38(1-2):31–53.
[52] Pollard D, Thompson SL. Use of a land-surface-transfer scheme (LSX) in a global climate model: the response to doubling stomatal resistance. Glob Planet Change 1995;10:129–61.
[53] Prihodko L, Denning AS, Baker I. Modelling drought tolerance in Amazonia with SiB3. In: Proceedings of the seventh international carbon dioxide conference. September 25–30, Boulder, Colorado; 2005. p. 683–4.
[54] Radcliffe D, Hayden T, Watson K, Crowley P, Phillips RE. Simulation of soil-water the root zone of a corn crop. Agron J 1980;72:19–24.
[55] Ronda RJ, De Bruin HAR, Holtslag AAM. Representation of the canopy conductance in modeling the surface energy budget for low vegetation. J Appl Meteorol 2001;40:1431–44.
[56] Rouse WR, Blyth EM, Crawford RW, Gyakum JR, Janowicz JR, Kochtubajda B, et al. Energy and water cycles in a high latitude, north-flowing river system: summary of results from the Mackenzie GEWEX study – phase 1. Bull Amer Meteor Soc 2002;84:73–87.
[57] Schulze ED, Kelliher FM, Korner C, Lloyd J. Relationships among maximum stomatal conductance, ecosystem surface conductance, carbon assimilation rate, and plant nitrogen nutrition: a global ecology scaling exercise. Ann Rev Ecol Sys 1994;25:629–60.
[58] Stahl K. Influence of hydroclimatology and socioeconomic conditions on water-related international relations. IWRA 2005;30:270–82.
[59] Steele SJ, Gower ST, Vogel JG, Norman JM. Root mass, net primary production and turnover in aspen, jack pine and black spruce forests in Saskatchewan and Manitoba, Canada. Tree Physiol 1997;17:577–87.
[60] Strong WL, La Roi GH. Rooting depths and successional development in selected boreal forest communities. Can J Forest Res 1983;13:577–88.
[61] Twine TE, Kustas WP, Norman JM, Cook DR, Houser PR, Meyers TP, et al. Correcting eddy-covariance flux underestimates over a grassland. Agr Forest Meteorol 2000;103:279–300.
[62] Van Drecht G, Bouwman AF, Boyer EW, Green P, Siebert S. A comparison of global spatial distributions of nitrogen inputs for nonpoint sources and effects on river nitrogen export. Glob Biogeochem Cycles 2005;19. doi:10.1029/2005GB002454.
[63] Vorosmarty CJ, Green P, Salisbury J, Lammers RB. Global water resources: vulnerability from climate change and population growth. Science 2000;289:284–8.
[64] Walko RL, Band LE, Baron J, Kittel TGF, Lammers R, Lee TJ, et al. Coupled atmosphere-biophysics-hydrology models for environmental modeling. J Appl Meteorol 2000;39:931–44.
[65] Ward AD, Trimble S. Environmental hydrology. CRC Press; 2004. p. 448.
[66] Williams TG, Flanagan LB. Measuring and modelling environmental influences on photosynthetic gas exchange in Sphagnum and Pleurozium. Plant Cell Environ 1998;21:555–64.
[67] Wilson KB, Baldocchi DD, Aubinet M, Berbigier P, Bernhofer Ch, Dolman H, et al. Surface energy partitioning between latent and sensible heat flux at FLUXNET sites. Water Resour Res 2002;38. doi:10.1029/2001 WR 000989.
[68] Wilson KB, Hanson PJ, Mulholland P, Baldocchi DD, Wullschleger S. A comparison of methods for determining forest evapotranspiration and its components: sap flow, soil water budget, eddy covariance and catchment water balance. Agr Forest Meteorol 2001;106:153–68.
[69] Zhang L, Dawes WR, Walker GR. Response of mean annual evapotranspiration to vegetation changes at catchment scale. Water Resour Res 2001;37:701–8.